8th International Symposium on Magnetic Bearing
August 26-28, 2002, Mito, Japan

BEARINGLESS HYDROGEN BLOWER

Rainer Baumschlager
Laboratory of Electrical Engineering and Design, ETH Zurich, 8005 Zurich, Switzerland
baumschlager@eek.ee.ethz.ch

Dr. Reto Schöb
Levitronix GmbH, 8005 Zurich, Switzerland
schoeb@levitronix.com

Dr. Joachim Schmied
Delta JS AG, 8005 Zurich, Switzerland
jschmied@delta-js.ch

ABSTRACT

This paper describes the progress made in a feasibility study on a bearingless hydrogen blower with a magnetically levitated drive system. Striving for compactness paired with the low density of hydrogen indicates high operating speeds.
The theoretical part of this study has been subdivided into three steps: Preliminary design of a radial compressor suitable for this application, layout of a corresponding high speed bearingless slice motor and a mechanical study on rotordynamic modelling including analysis of the dynamic behaviour and investigations of further mechanical questions.
Alongside these theoretical investigations a prototype test rig with a nominal speed of 56000 *rpm* was operated to gain practical experience.
Alternative approaches were also studied because severe problems were encountered in the mechanical study and in the experiments.

INTRODUCTION

In the recent two decades research in electric drives and magnetic bearings have led to the so-called bearingless motor ([2], [5], [10] and [15]). In contrast to conventional drives (with common bearings or magnetic bearings) the bearingless motor generates the magnetic bearing forces in the motor itself. A bearingless motor usually requires two bearing-motor parts to stabilise the rotor in five degrees of freedom (the sixth degree of freedom is the drive's rotation).
To cut on length and system complexity, the bearingless slice motor has been developed in a joint project of the ETH Zurich and Levitronix GmbH in Zurich, Switzerland ([1], [14] and [16]).
Based on this technology a bearingless centrifugal hydrogen blower prototype has been designed which allows rotating and pumping without common bearings or seals[1]. The basic principle is illustrated in Figure 1: A rotor slice is suspended und driven in the magnetic fields of a stator without mechanical contact. The pump head consists of two main parts: the bearing drive rotor with plastic impeller, and the pump casing. A digital signal processor system with a servo amplifier allows precise regulation of the speed, pressure or flow rate. Because of the unique combination of active (radial displacement and rotation) and passive (axial displacement and tilting) magnetic forces, the system costs can be kept at a minimum.

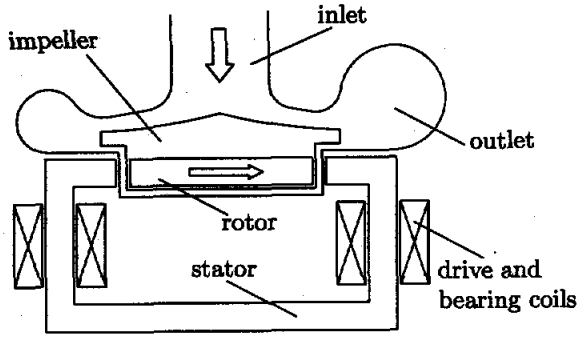

FIGURE 1: Schematic of the basic principle of the bearingless centrifugal blower

[1]Auxiliary ball bearings have been included in the prototype design as back-up only.

TABLE 1: Blower performance

Description	Symbol	Value	Dim.
Rotational speed	n	56000	rpm
Mass flow	$\frac{dm}{dt}$	18	g/s
Pressure ratio	$\Pi = \frac{p_{out}}{p_{in}}$	1.14	
Mech. input power	P_{mech}	850	W
Total efficiency	η_t	0.52	
Work coefficient	μ_0	0.85	
Flow coefficient	ϕ	0.0075	

DESIGN

This section describes the component design of the prototype blower.

Blower design

A preliminary design of the radial compressor stage (impeller, diffuser and volute) has been carried out. The impeller has been designed using a one-dimensional analysis to identify the effect of various design parameters. This has been followed by a quasi-three dimensional design using standard radial compressor design tools [3], [4].

An impeller with an extremely low flow coefficient

$$\phi = \frac{\dot{V}}{u_2 D_2^2} = 0.0075$$

(with $\dot{V}$: volume flow, u_2: circumferential speed at the impeller outlet and D_2: impeller diameter) at the lower end of the feasible range for a radial stage has been proposed.

The diffuser has been selected from experience with similar coefficient stages and a publication on low solidity diffusers [7]. A standard one-dimensional method has been used for the design of the volute.

The estimated performance in the design point is listed in Table 1. The impeller has six blades, 6 splitter vanes and an outlet diameter of $D_2 = 80\ mm$ (Figure 2), and is used together with a relatively short low-solidity bladed diffuser and a conventional volute. Figure 3 illustrates the components of the blower.

Magnetic circuit and motor design

For the experiments an off the shelf bearingless slice motor has been used that was modified for experimental high speed operation. The stator iron is set up as a so-called temple motor [1]. With this setup, the iron losses become too high for permanent operation at high speeds.

Aiming for minimised losses, two radial bearingless drive concepts were designed and their performances were evaluated theoretically. The required gas compression and mass flow demand a motor with the

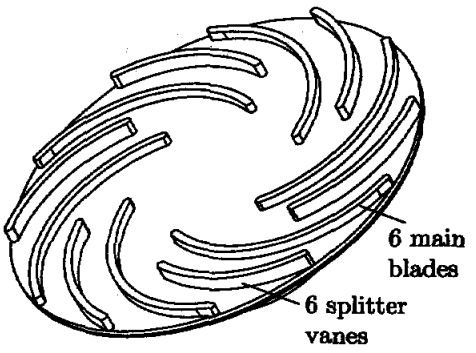

FIGURE 2: Impeller hub with blades

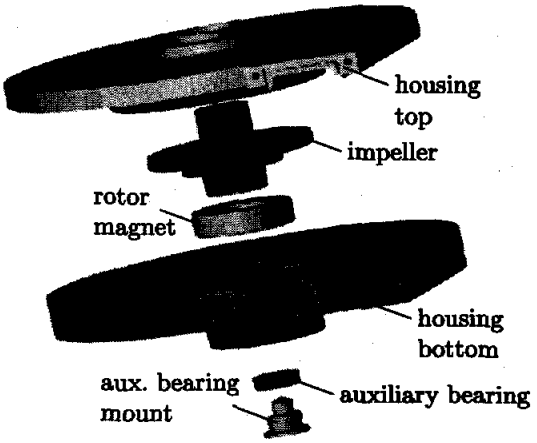

FIGURE 3: Exploded view of the blower

TABLE 2: Motor data

Description	Symbol	Value	Dim.
Mechanical power	P_{mech}	1100	W
Rotational speed	n	58000	rpm
Motor torque	M	18.1	Ncm
Radial forces	F	9.75	N
DC-link voltage	U_{dcl}	72	V

parameters summarised in Table 2. The data exceed the requirements stated in Table 1 to obtain motor designs with reserves.

Different materials have been considered for the electromagnetic circuit to minimise losses.

Materials considerations

The process gas consists of the components H_2, N_2 and H_2O. Materials in discussion for the rotor and the impeller are PEEK polymer and stainless steel. Certain materials can become brittle in an hydrogen environment and small cracks can eventually arise. The mechanism for this effect is a chemical reaction of hydrogen ions (H^+) with carbon (C) to methane (CH_4). The methane molecules require more space which causes internal stresses and sub-sequently the

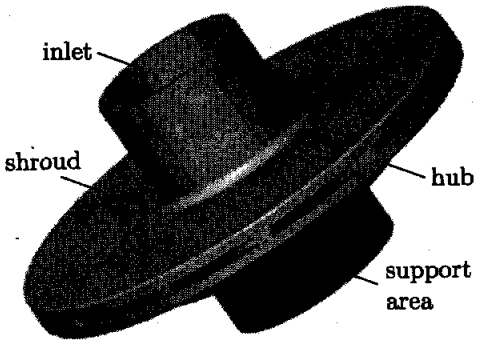

FIGURE 4: Impeller of the blower

TABLE 3: Nominal material data of PEEK

Description	Symbol	Value	Dim.
Density	ρ_{H_2}	1320	kg/m^3
Young's modulus	E	3600	MPa
Poisson's ratio	ν	0.5	
Yield strength	σ_{max}	96	MPa

material becomes brittle.
The creation of hydrogen ions is encouraged by high temperatures, high pressures and high velocities with which the gas hits the material surface. Rough limits are pressures higher than 30 bar and temperatures higher than 80 $°C = 353\ K$. The present application has a much lower pressure and slightly lower temperatures than these limits.
Most steels contain free C and are therefore prone to become brittle in an H_2 environment with high temperature and pressure. Alloys containing materials with a high affinity to carbon such as chromium or molybdenum are less prone.
Most plastics do not have free carbon and should therefore be resistant in an H_2 environment. According to a PEEK manufacturer none of the gas components (H_2, N_2 and H_2O) will cause any chemical attack to PEEK, although the small H_2 molecules might penetrate the PEEK matrix.
PEEK has been chosen as the impeller material for these reasons.

MECHANICAL FEASIBILITY

This section covers the estimation of mechanical stresses, investigations on the rotor dynamics and a prediction of the drop-down behaviour of the proposed bearingless slice motor.

Estimation of mechanical stresses

The components of the impeller are labelled in Figure 4. The stresses are estimated assuming standard material data for PEEK (see Table 3), plane stress

TABLE 4: σ_t : tangential stress; σ_r : radial stress

Location	Inner/outer diameter	Max. stress
Inlet	22/26 mm	$\sigma_t = 8.4\ MPa$
Shroud	22/80 mm	$\sigma_t = 70\ MPa$
Hub	0/80 mm	$\sigma_t = 34\ MPa$
		$\sigma_r = 34\ MPa$
Support area	22/30 mm	$\sigma_t = 11\ MPa$

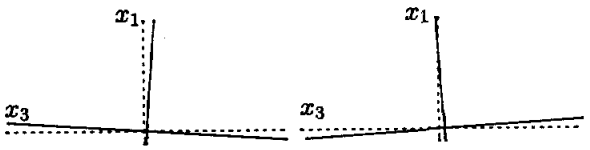

mode shape 1: tilting ($34.24\ Hz$) mode shape 2: parallel ($45.554\ Hz$)

FIGURE 5: Impeller mode shapes, $n = 0\ rpm$

condition and considering each of the four sectors impeller inlet, impeller shroud[2], impeller hub and impeller support[3] as separate cylinders or disks, respectively. This gives a good overview of the general stress level. For local peak stresses a finite element analysis would be necessary. Table 4 summarises the stresses due to the centrifugal load at a speed of 60000 rpm.
The formulae for the radial and tangential stresses of a rotating disk can be found in [7]. For the disc with a hole, the maximum stress is the tangential stress at the inner diameter

$$\sigma_t(r_1) = \left(0.824 + 0.175\frac{r_1}{r_2}\right)\rho u_2^2$$

with r_1: inner radius, r_2: outer radius, ρ: density and u_2: circumferential speed at outer diameter.

Rotor dynamics

The natural mode shapes and frequencies of the directly supported impeller at standstill as well as at full speed are illustrated in Figure 5 and in Figure 6, respectively. For the radial stiffness, which is determined by the magnetic bearing controller, a value according to the bearing specification has been assumed.
Due to the extreme gyroscopic effect at full speed the backward tilting mode drops to a very low frequency, whereas the forward mode (the so called nutation) rises to very high values, approximately proportional to

$$\frac{\Theta_p}{\Theta_a} n$$

[2]The hub supports the shroud against the centrifugal load; the load due to the blades is neglected.
[3]The magnetic ring at the outer diameter supports the impeller against the centrifugal load.

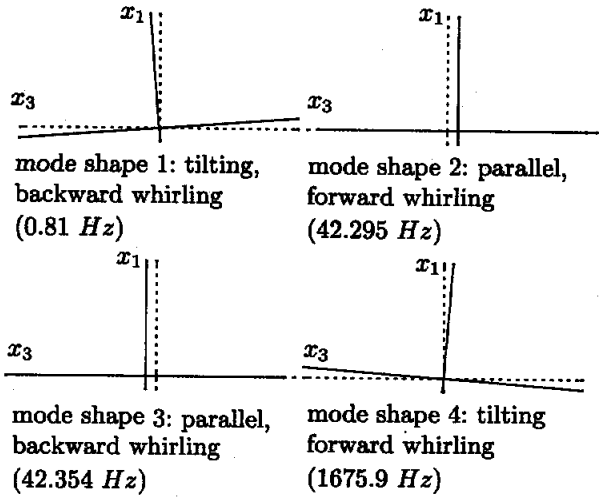

FIGURE 6: Impeller mode shapes, $n = 60000\ rpm$

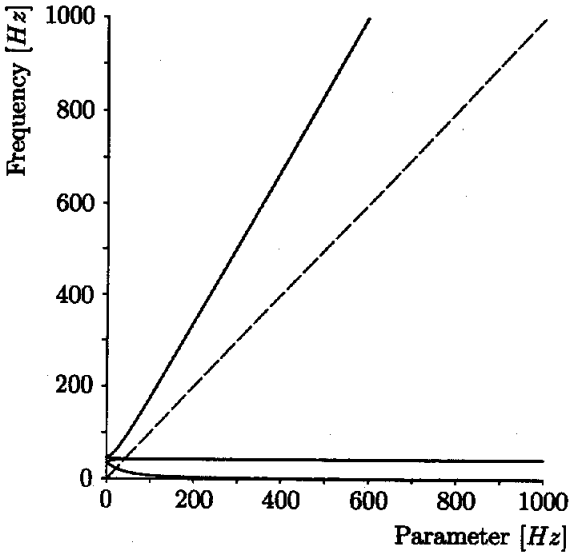

FIGURE 7: Natural frequencies as a function of speed

with Θ_p: polar moment of intertia and Θ_a: transversal moment of intertia. The given relation is valid for the free unsupported rotor.
The natural frequencies as a function of speed can be seen in Figure 7. There are two modes at standstill. Each of theses splits up into a forward and a backward mode when the rotor starts to rotate. The speed line crosses three mode lines; i.e. there are three critical modes. However, the backward modes cannot be excited by rotor unbalance. Hence, only one critical speed is expected at run-up.

The very low frequency of the backward tilting mode causes two problems:
The low frequency indicates, that the rotor almost behaves as if not supported, hence it is very sensitive to any transient base acceleration. Therefore allowable base accelerations at low frequencies are limited.
Depending on the implementation, the integrator of the radial bearing controller can cause negative phase angles of the transfer function at low frequencies. Hence the mode can be unstable. This problem can be solved by using a first order low pass filter instead of an integrator (see MEDYN controller building blocks in [12]).
The rising frequency of the forward tilting mode causes another problem: The radial bearing controller must provide damping at every frequency up to 1676 Hz. Due to the phase lag of the amplifier, the digitisation and the time delay of the processor this is not possible. Therefore two controllers are necessary: One for low speeds, when this mode still has a low frequency and the damping can be created by phase lead, the other for high speeds, where damping can only be achieved with a phase angle below 180° by means of a second order filter [11].
The Figures 5 to 7 were calculated with the rotordynamics software package MADYN [9]. To investigate the closed loop system stability, the software add-on MEDYN can be used [12].

Drop-down behaviour

A rotor in its auxiliary bearings can only whirl with a frequency below the natural frequency of the rotor in the auxiliary bearings ($\Omega_{whirl} < \Omega_0$). Otherwise the equilibrium of forces at contact is not fulfilled [13]. The natural frequency

$$\Omega_0 = \sqrt{\frac{2k_{aux_{bearing}}}{m_{rotor}}} \tag{1}$$

is therefore an upper limit for the whirl frequency. The natural frequency in auxiliary bearings is determined by their stiffness: According to [8] the stiffness in N/m of ball bearings can be calculated as

$$k_{aux_{bearing}} = 1.3 \cdot 10^6 \sqrt[3]{z^2 D_{ball} F} \tag{2}$$

with z: number of balls, D_{ball}: ball diameter $[mm]$ and F: bearing force $[N]$.
When whirling occurs the bearing load is

$$F = m_{rotor} r \Omega_{whirl}^2 \tag{3}$$

with m: rotor mass and r: whirl radius. Equations 1 to 3 can be solved for the bearing force

$$F = 4.19 \cdot 10^9 z \sqrt{r^3 D_{ball}}$$

The auxiliary bearing clearance is a good approximation for the whirl radius r. Choosing $r = 0.1\ mm$

yields $F \approx 100\ kN$. This result is beyond the capacity of normal ball bearings.
However, the estimation represents the worst case scenario; there is no damping in the model. If the forces are damped the problem will get less critical.
As mentioned before, the calculated whirl frequency is the utmost limit.
Summing up, in this mechanical study two major concerns were found:
The low frequency and damping of the backward whirling mode at high operating frequencies.
The extremely high forces which might potentially act on the auxiliary bearing in case of whirl motion during drop-down.

EXPERIMENTAL INVESTIGATIONS

Since it was not possible to judge the relevance of the issues pointed out in the mechanical feasibility study by further theoretical investigations, it was decided to implement an experimental prototype: The blower housing was manufactured with rapid prototyping and the impeller was traditionally machined. A standard bearingless slice motor was modified for operation at high speeds. That included special adjustment of the position sensors and adaption of the drive and bearing coils. Photographs of the high speed test rig can be seen in Figure 8 and in Figure 9.

Rotordynamic observations

A slow backward whirling motion could clearly be monitored at high rotational speeds with the test prototype. Since this mode could be easily excited by low frequency vibration, it would be a major concern for the application of this blower system.

Drop-down behaviour

The behavior of the rotor during drop-down was also studied with the same prototype at several speeds. As expected, no pure whirling motion but a rather chaotic motion was observed. It could be concluded that the auxiliary bearing forces would be much lower than those calculated in the worst case. However, during one test the forces were higher than the auxiliary bearings could handle and the test system was severely damaged.

ALTERNATIVE DESIGNS

Because of the mechanical problems related with the proposed design based on the bearingless slice motor, two alternative drive concepts were studied: First, a canned motor with a long shaft and two separated magnetic bearings was laid out for operation at a nominal speed of 56000 *rpm* (see Figure 10). Second, an ultra-high-speed motor with separate magnetic bearings was designed for a diagonal flow blower with a diameter of only $34mm$ and a rotational speed of 140000 *rpm* (see Figure 11).
Mechanical studies showed that both concepts are clearly feasible from a mechanical point of view and that the related rotordynamics problems are less delicate than with the bearingless slice motor. While concept one is straight forward but leads to a relatively large system, proposal two would be extremely small and compact but implies more uncertainties.

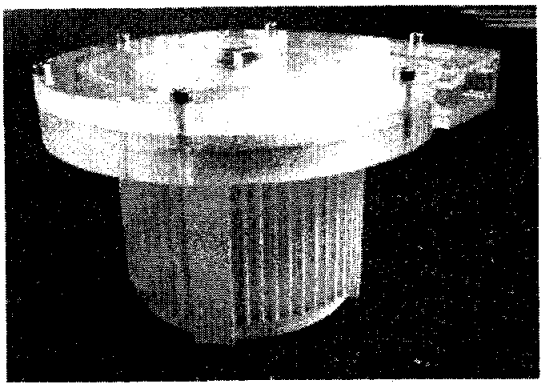

FIGURE 8: Front view of the prototype

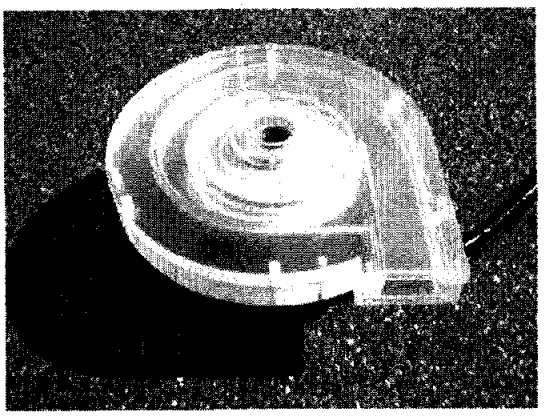

FIGURE 9: Top view of the prototype

CONCLUSIONS

It has been shown, that a simple and compact centrifugal blower stage with a nominal speed of 56000 *rpm* could fulfill the requirements for hydrogen compression.
A bearingless slice motor for such a blower proved to be feasible from the electrical, thermal and magnetic side. However, two mechanical problems have been detected with the proposed bearingless slice motor: Low damping of the backward whirling mode at low frequencies and extremely high auxiliary bear-

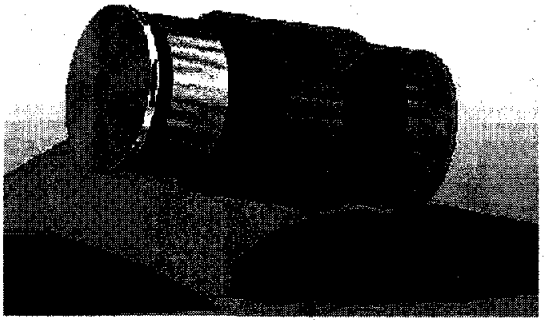

FIGURE 10: Proposed high speed concept (56000 *rpm*)

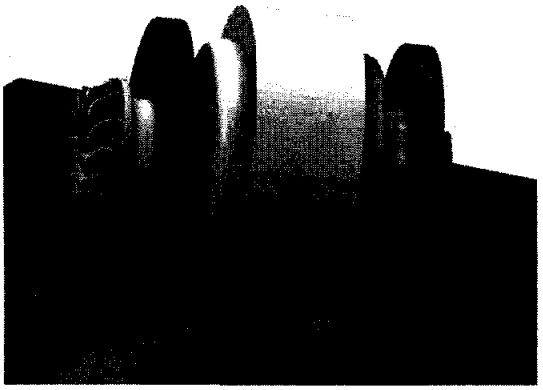

FIGURE 11: Proposed ultra high speed concept (140000 *rpm*)

ing forces.
Extensive work would have to be done to solve both problems satisfactory. Therefore the two alternative designs which have also been investigated seem to be more promising.

References

1. Barletta, N., Der lagerlose Scheibenmotor, Dissertation ETH No. 12870, Zurich, 1998.

2. Bichsel, J., Beiträge zum lagerlosen Elektromotor, Dissertation ETH No. 9303, Zurich, 1990.

3. Casey, M. V., A computational geometry for the blades and internal flow channels of centrifugal compressors, ASME Journal of Engineering for Power, Vol. 105, pp 288-295, April 1983.

4. Casey, M. V., and Roth, P., A streamline curvature through-flow method for radial turbocompressors, I. Mech. E. Conference on Computational Methods in Turbo-machinery, Birmingham, April 1984.

5. Chiba, A., Power, D. T., Rahman, M. A., Characteristics of a Bearingless Induction Motor, IEEE Transactions on Magnetics, Vol. 27, No. 6, November 1991.

6. Czichos, H., Hütte, Grundlagen der Ingenieurwissenschaften, 29. Auflage, Springer-Verlag, Berlin - Heidelberg, 1991.

7. Kmecl and Dalbert, ASME 99-GT, ASME Gas Turbine Conference, 1999.

8. Krämer, E., Dynamics of Rotors and Foundations, Springer-Verlag, Berlin - Heidelberg, 1993.

9. Manuals of the MADYN Finite Elements Program System, Version 4.2, 1998.

10. Ohishi, T., Okada, Y., and Dejima, K., Analysis and Design of a Concentrated Wound Stator for Synchoronous-Type Levitated Rotor, Fourth International Symposium on Magnetic Bearings, Zurich, 1994.

11. Schmied, J., and Betschon, F., Engineering for Rotors Supported on Magnetic Bearings: The Process and the Tools, Proceedings of the Sixth International Symposium on Magnetic Bearings, Boston, 1998.

12. Schmied, J., MEDYN, Functions for the Treatment of Mechatronic System's Dynamics, input description, Delta JS AG, Zurich, August 1999.

13. Schmied, J., Pradetto, J. C., Behaviour of a One Ton Rotor being Dropped into Auxiliary Bearings, Proceedings of the Third International Symposium on Magnetic Bearings, Alexandria VA, 1992.

14. Schöb, R., and Barletta, N., Principle and Application of a Bearingless Slice Motor, Fifth International Symposium on Magnetic Bearings, Kanazawa, 1996.

15. Schöb, R., Beiträge zur lagerlosen Asynchronmaschine, Dissertation ETH No. 10417, Zurich, 1993.

16. Silber, S., Amrhein, W., Bearingless Single-Phase Motor with Concentrated Full Pitch Windings in Exterior Rotor Design, Sixth International Symposium on Magnetic Bearings, Cambridge MA, 1998.